Spontaneous Formation of Vesicles and Dispersed Cubic and Hexagonal Particles in Amino Acid-Based Catanionic Surfactant Systems

Mónica Rosa,*,†,‡ Maria Rosa Infante,§ Maria da G. Miguel,‡ and Björn Lindman†

Physical Chemistry 1, Lund University, P.O. Box 124, 22100 Lund, Sweden, Chemistry Department, Coimbra University, 3004-535 Coimbra, Portugal, and Department of Surfactant Technology, IIQAB-CSIC, J. Girona 18-26, 08034 Spain

Received December 22, 2005. In Final Form: April 5, 2006

Mixed catanionic surfactant systems based on amino acids were investigated with respect to the formation of liquid crystal dispersions and the stability of the dispersions. The surfactants used were arginine-*N*-lauroyl amide dihydrochloride (ALA) and N^{α}-lauroyl-arginine-methyl ester hydrochloride (LAM), which are arginine-based cationic surfactants; sodium hydrogenated tallow glutamate (HS), a glutamic-based anionic surfactant; and the anionic surfactants sodium octyl sulfate (SOS) and sodium cetyl sulfate (SCS). It is demonstrated that in certain ranges of composition there is a spontaneous formation of vesicular, cubic, and hexagonal structures. The solutions were characterized with respect to internal structure and size by cryogenic transmission electron microscopy (cryo-TEM), dynamic light scattering (DLS), and turbidity measurements. Vesicles formed spontaneously and were found for all systems studied; their size distribution is presented for the systems ALA/SCS/W and ALA/SOS/W; they are all markedly polydisperse. The aging process for the system ALA/SOS/W was monitored both by turbidity and by cryo-TEM imaging; the size distribution profile for the system becomes narrower and the number average radius decreases with time. The presence of dispersed particles with internal cubic structure (cubosomes) and internal hexagonal structure (hexosomes) was documented for the systems containing ALA and HS. The particles formed spontaneously and remained stably dispersed in solution; no stabilizer was required. (Cubosome and hexosome are USPTO registered trademarks of Camurus AB, Sweden.) The spontaneous formation of particles and their stability, together with favorable biological responses, suggests a number of applications.

Introduction

Interest in dispersed surfactant and lipid liquid crystalline phases has increased strongly in recent years, and they are starting to be used in several applications. Scientists have known about vesicles for a long time, and their similarity with cell membranes as well as their apparent capability of carrying cargo early on triggered the attention of the scientific community. Consequently, a large number of systems have been developed and studied, including in their compositions naturally occurring lipids,[1,2] double-chained surfactants,[3−5] and several kinds of mixed surfactants (nonionic, cationic and/or anionic, double and/or single tailed), some of them having grafted polymers.[6−12] Nowadays, they are used in quite a large number of applications: drug and gene delivery systems, cosmetic and food formulations, models for membranes, microreactors, and substrates for a variety of enzymes and proteins, among others.[13]

Cubosomes are dispersions of a cubic liquid crystalline phase and are thus particles with an internal cubic structure, whereas vesicle solutions are often dispersions of a lamellar phase. Dispersed cubic structures were first detected in nature in the late 1960s by Donnay and Pawson;[14] after removal of the organic matrix from the echinoderm skeleton, a cubic structure was found. Patton and Carey[15] also found cubic structures in the process of fat digestion by human pancreatic lipase. However, the first synthetic cubosomes were recognized when studying the phase behavior of unsaturated monoglycerides (uMGs);[16] later it was discovered that the uMG cubic structure could be dispersed into micrometer-sized particles by mechanical breakup in the presence of micellar solutions of bile salts or caseins.[17,18] Some years afterward, Landh[19] realized that amphiphilic block copolymers stabilized these dispersed particles. The aim soon became to make the smallest and most monodisperse particles possible; techniques such as ultrasonication, homogenization, and emulsification[20−25] were applied.

* Corresponding author. E-mail: monica.rosa@fkem1.lu.se.
† Lund University.
‡ Coimbra University.
§ IIQAB-CSIC.

(1) Hargreaves, W. R.; Deamer, D. W. *Biochemistry* **1978**, *17*, 3759−3768.
(2) Gabriel, N. E.; Roberts, M. F. *Biochemistry* **1984**, *23*, 4011−4015.
(3) Talmon, Y.; Evans, D. F.; Ninham, B. W. *Science* **1983**, *221*, 1047−1048.
(4) Brady, J. E.; Evans, D. F.; Kachar, B.; Ninham, B. W. *J. Am. Chem. Soc.* **1984**, *106*, 4279−4280.
(5) Miller, D. D.; Bellare, J. R.; Kaneko, T.; Evans, D. F. *Langmuir* **1988**, *4*, 1363−1367.
(6) Kaler, E. W.; Murthy, A. K.; Rodriguez, B. E.; Zasadzinski, J. A. N. *Science* **1989**, *245*, 1371−1374.
(7) Kaler, E. W.; Herrington, K. L.; Murthy, A. K.; Zasadzinski, J. A. N. *J. Phys. Chem.* **1992**, *96*, 6698−6707.
(8) Yatcilla, M. T.; Herrington, K. L.; Brasher, L. L.; Kaler, E. W.; Chiruvolu, S.; Zasadzinski, J. A. *J. Phys. Chem.* **1996**, *100*, 5874−5879.
(9) Marques, E. F.; Regev, O.; Khan, A.; Miguel, M. D.; Lindman, B. *J. Phys. Chem. B* **1998**, *102*, 6746−6758.
(10) Marques, E. F.; Regev, O.; Khan, A.; Miguel, M. D.; Lindman, B. *J. Phys. Chem. B* **1999**, *103*, 8353−8363.
(11) Villeneuve, M.; Kaneshina, S.; Imae, T.; Aratono, M. *Langmuir* **1999**, *15*, 2029−2036.
(12) Joannic, R.; Auvray, L.; Lasic, D. D. *Phys. Rev. Lett.* **1997**, *78*, 3402−3405.
(13) Lasic, D. D. *Trends Biotechnol.* **1998**, *16*, 307−321.
(14) Donnay, G.; Pawson, D. L. *Science* **1969**, *166*, 1147.
(15) Patton, J. S.; Carey, M. C. *Science* **1979**, *204*, 145−148.
(16) Lindström, M.; Ljusberg-Wahren, H.; Larsson, K.; Borgström, B.. *Lipids* **1981**, *16*, 749−754.
(17) Buchheim, W.; Larsson, K. *J. Colloid Interface Sci.* **1987**, *117*, 582−583.
(18) Larsson, K., *J. Phys. Chem.* **1989**, *93*, 7304−7314.
(19) Landh, T. *J. Phys. Chem.* **1994**, *98*, 8453−8467.
(20) Nakano, M.; Sugita, A.; Matsuoka, H.; Handa, T. *Langmuir* **2001**, *17*, 3917−3922.
(21) Nakano, M.; Teshigawara, T.; Sugita, A.; Leesajakul, W.; Taniguchi, A.; Kamo, T.; Matsuoka, H.; Handa, T. *Langmuir* **2002**, *18*, 9283−9288.

10.1021/la053464p CCC: $33.50
Published on Web 05/27/2006

Some other ways of making cubosomes are being studied in order to facilitate their preparation for industrial purposes, for example, through the inclusion of a hydrotrope[26] or the use of dry powder precursors.[27] In the former process,[26] the introduction of ethanol into the system and the choice of an appropriate dilution pathway in the ternary phase diagram resulted in cubic dispersions without laborious fragmentation processes. In the latter one,[27] two types of dry powder cubosome precursors produced by spay-drying were presented; starch- and dextran-based encapsulants are used to decrease powder cohesion during drying and to act as a soluble colloidal stabilizer upon hydration of the powders.

Hexosomes are also dispersed particles with internal structure that in this case is hexagonal. Hexosomes were imaged for the first time by Gustafsson et al.[28] The addition of a lipophilic additive, retinyl palmitate, to the glycerol monooleate-based cubic structure results in the formation of a reversed hexagonal structure,[29] which can be dispersed by the addition of stabilizers.[30,31] More recently, further dispersed hexagonal particles have been presented (i.e., in a monolinolein/water[32] and a monolinolein/tetradecane/water[33] system, where a reversible transition from cubic via hexagonal to fluid isotropic can be tuned by temperature, and in a mixture of diglycerol monooleate and glycerol dioleate in water[34]). All of these studies were performed in the presence of a polymer-based stabilizer.

The identification of these nonlamellar structures in biological systems has motivated considerable work to characterize them as well as to try to understand their role in the cellular mechanisms where they participate. They are now believed to play an important role as transient structures in complex processes such as membrane fusion[35,36] and the formation of cell−cell contacts through tight junctions.[37] Their colloidal, chemical, biocompatible, biodegradable, and surface properties provide a whole range of possibilities from gene and drug carriers (antifungal, anticancer agents, vaccines) and cosmetic formulations (skin care, shampoos) to diagnostic and various uses in the food industry.

In our work, amino acid-based catanionic systems of single-tailed surfactants are presented. We used arginine- and glutamate-based surfactants: arginine-*N*-lauroyl amide dihydrochloride (ALA) and N^{α}-lauroyl-arginine-methyl ester hydrochloride (LAM) are arginine-based cationic surfactants with two and one positive charges per headgroup, respectively; sodium hydrogenated tallow glutamate (HS) is a glutamate-based double charged anionic surfactant. Our studies were to a great extent motivated by the belief that amino acid-based compounds would be much better tolerated by biological systems than conventional cationic surfactants. Indeed cell viability tests performed proved this to be right; LAM, ALA, and HS presented cell viability percentages above 90% (results to be published). ALA and LAM have also been reported as being biodegradable;[38] this is also a relevant feature for a number of applications. Our work focused on mixed systems between these two amino acid-based cationic surfactants and different anionic surfactants, which also included sodium octyl and cetyl sulfate, SOS and SCS, respectively.

By catanionic surfactants we understand mixtures of cationic and anionic amphiphiles. Several catanionic surfactant mixtures have been studied, and vesicles were generally found to form spontaneously.[6−10]

Catanionic mixtures are known to present intriguing phase behavior, a spontaneous formation of vesicles being one of their characteristics, together with the indication that the vesicles formed are close to thermodynamic stability. For the systems studied here, the spontaneous formation of vesicles was one of the observations. In addition, cubosomes and hexosomes were visualized for the completely amino acid-based system (i.e., mixtures of arginine- and glutamate-based surfactants). These systems are hoped to represent a step forward from a scientific and application point of view first because of the growing need to present new nontoxic and biodegradable systems and second because of the importance of exploring new systems displaying novel properties.

For all cubosome and hexosome systems presented so far in the literature, the presence of a stabilizer was crucial for these dispersed structures to be formed.[19,31] This is not the case for the systems presented here where no stabilizer was needed; the particles formed spontaneously and remained stably dispersed in solution for long times.

Experimental Section

Materials. Sodium octyl and cetyl sulfate (SOS and SCS) were obtained from Merck and used as received. Sodium hydrogenated tallow glutamate (HS), a glutamic-based anionic surfactant, was obtained as a gift from Ajinomoto[39,40] and was recrystallized from ethanol before use. Regarding arginine-*N*-lauroyl amide dihydrochloride (ALA) and N^{α}-lauroyl-arginine-methyl ester hydrochloride (LAM), their synthesis and physicochemical properties can be found in the literature.[38,41,42] ALA and HS have two charges in the headgroup, positive and negative, respectively. All concentrations are presented per charge. Water was purified using a Millipore Q system.

Sample Preparation. Solutions of catanionic vesicles were prepared by making stock solutions of individual surfactants, combining them, at the desired concentrations, with the required amount of water, and mixing all components by simple hand agitation. Then, they were left to equilibrate at 25 °C for a few days. The sample compositions of all systems selected for this study are reported in Table 1.

Turbidity Measurements. Turbidity measurements were performed for the vesicle systems ALA/SCS/W and ALA/SOS/W at 25 °C. A Lambda14 UV/vis spectrometer (Perkin-Elmer) was used, at the wavelength of 400 nm, using a 0.5 cm path length quartz cell. For the system ALA/SCS/W, turbidity experiments were also

(22) Siekman, B.; Bunjes, H.; Koch, M. H. J.; Westesen, K. *Int. J. Pharm.* **2002**, *244*, 33−43.
(23) Esposito, E.; Eblovi, N.; Rasi, S.; Drechsler, M.; Di Gregorio, G. M.; Menegatti, E.; Cortesi, R. *AAPS Pharm. Sci.* **2003**, *5*, A30.
(24) Barauskas, J.; Johnsson, M.; Joabsson, F.; Tiberg, F. *Langmuir* **2005**, *21*, 2569−2577.
(25) Barauskas, J.; Johnsson, M.; Tiberg, F. *Nano Lett.* **2005**, *5*, 1615−1619.
(26) Spicer, P. T.; Hayden, K. L.; Lynch, M. L.; Ofori-Boateng, A.; Burns, J. L. *Langmuir* **2001**, *17*, 5748−5756.
(27) Spicer, P. T.; Small, W. B.; Lynch, M. L.; Burns, J. L., *J. Nanopart. Res.* **2002**, *4*, 297−311.
(28) Gustafsson, J.; Arvidson, G.; Karlsson, G.; Almgren, M. *Biochim. Biophys. Acta* **1995**, *1235*, 305−312.
(29) Caboi, F.; Amico, G. S.; Pitzalis, P.; Monduzzi, M.; Nylander, T.; Larsson, K. *Chem. Phys. Lipids* **2001**, *109*, 47−62.
(30) Gustafsson, J.; LjusbergWahren, H.; Almgren, M.; Larsson, K. *Langmuir* **1996**, *12*, 4611−4613.
(31) Gustafsson, J.; Ljusberg-Wahren, H.; Almgren, M.; Larsson, K. *Langmuir* **1997**, *13*, 6964−6971.
(32) deCampo, L.; Yaghmur, A.; Sagalowicz, L.; Leser, M. E.; Watzke, H.; Glatter, O. *Langmuir* **2004**, *20*, 5254−5261.
(33) Yaghmur, A.; deCampo, L.; Sagalowicz, L.; Leser, M. E.; Glatter, O. *Langmuir* **2005**, *21*, 569−577.
(34) Johnsson, M.; Lam, Y.; Barauskas, J.; Tiberg, F. *Langmuir* **2005**, *21*, 5159−5165.
(35) Chernomordik, L. *Chem. Phys. Lipids* **1996**, *81*, 203−213.
(36) Luzzati, V. *Curr. Opin. Struct. Biol.* **1997**, *7*, 661−668.
(37) Wegener, J.; Galla, H.-J. *Chem. Phys. Lipids* **1996**, *81*, 229−255.
(38) Moran, C.; Clapes, P.; Comelles, F.; Garcia, T.; Perez, L.; Vinardell, P.; Mitjans, M.; Infante, M. R. *Langmuir* **2001**, *17*, 5071−5075.
(39) Takehara, M.; Takizawa, K.; Yoshimur. I.; Yoshida, R. *J. Am. Oil Chem. Soc.* **1972**, *49*, 157−.
(40) Takehara, M.; Yoshida, R.; Yoshimur. I.; Moriyuki, H. *J. Am. Oil Chem. Soc.* **1972**, *49*, 143−.
(41) Infante, M. R.; Pinazo, A.; Seguer, J. *Colloids Surf., A* **1997**, *123*, 49−70.
(42) Moran, C.; Pinazo, A.; Clapes, P.; Perez, L.; Vinardell, P.; Infante, M. R. *Green Chem.* **2004**, *6*, 233−240.

Table 1. Experimental Compositions of the Selected Systems Studied[a]

system	sample	[S^+]	[S^-]	wt % W	*R*	observations
LAM/SCS/W	1	15.6	10.6	99.00	1.5	vesicles, rods, and lamella
	2	3.9	2.6	99.75	1.5	vesicles, rods, and disks
	3	2.7	1.8	99.83	1.5	vesicles, rods, and lamella
	4	1.6	1.0	99.90	1.5	vesicles, rods, and disks
ALA/SCS/W	5	43.6	17.4	98.50	2.5	rods and vesicles
	6	46.3	15.8	98.50	2.9	rods and vesicles
	7	30.9	10.6	99.00	2.9	rods and vesicles
	8	15.4	5.3	99.50	2.9	vesicles
ALA/SOS/W	9	58.2	34.4	98.00	1.7	vesicles
	10	46.3	23.5	98.50	2.0	vesicles and rods
	11	29.1	17.2	99.00	1.7	vesicles
	12	30.9	15.6	99.00	2.0	vesicles and rods
ALA/HS/W	13	13.5	10.2	99.50	1.3	cubosomes and hexosomes
	14	2.2	1.6	99.92	1.3	cubosomes and vesicles

[a] The following abbreviations are used: ALA for arginine-*N*-lauroyl amide dihydrochloride; LAM for N^{α}-lauroyl-arginine-methyl ester hydrochloride; SCS (SOS) for sodium cetyl (octyl) sulfate; and HS for sodium hydrogenated tallow glutamate. *R* is the molar ratio between the cationic and anionic surfactant. All concentrations are presented in mM on a charge basis. Note that ALA and HS have two charges per molecule.

performed at 40 °C; a Haake Fisons K20 temperature controller was used. Experiments were performed at intervals of about 8 days for 24 days.

Cryogenic Transmission Electron Microscopy (cryo-TEM). Cryo-TEM is a powerful technique for the direct visualization of colloidal aggregates in aqueous media, provided particle sizes range from 5 to 10 nm to 1 μm. Controlled sample preparation conditions are required: a controlled-environment vitrification system (CEVS), at controlled temperature (to prevent temperature changes) and humidity (to minimize water loss), was used.[43] Vitrified samples were prepared and imaged according to a procedure described in the literature.[43−45] A Philips CM 120 Bio-Twin microscope equipped with a postcolumn energy filter, using an Oxford CT3500 cryoholder and its workstation, was used. All images were recorded digitally through a CCD camera (Gatan MSC791).

Dynamic Light Scattering. The setup for dynamic light scattering (DLS) is an ALV/DLS/SLS-5000F, CGF-8F-based compact goniometer system from ALV-GmbH (Langen, Germany).The light source is a CW diode-pumped Nd:YAG solid-state Compass-DPSS laser with symmetrizer from Coherent, Inc. (Santa Clara, CA). It operates at 532 nm with a fixed output power of 400 mW. Perfect vertical polarization is achieved using a Glan-Thomson laser polarizer prism with a polarization ratio of better than 105 in front of the cell housing. The scattering cells were immersed in a cylindrical quartz container (a vat) that is filled with a refractive index matching liquid (decalin and toluene, for experiments at 22 and 40 °C, respectively). The vat is positioned in a thermostated cell housing. The temperature of the vat can be varied from −12 to +140 °C and is controlled to ±0.01 °C by an F32 Julabo heating circulator. The goniometer has a range of scattering angles (θ) between 12 and 155°. The unpolarized scattered light is collected using a near-monomodal optical fiber and two matched photomultipliers that are put in a pseudo-cross-correlation arrangement. For DLS measurements using photon correlation spectroscopy, two multiple τ digital correlators, ALV-5000/E and ALV-5000/FAST Tau Extension, with a total of 320 exponentially spaced channels are employed to produce the time correlation function of the scattered intensity, $G^{(2)}(t)$ (auto or pseudo-cross), with an initial real sampling time of 12.5 ns. For DLS measurements, about 1 mL of the vesicle solution was added directly to the cylindrical light scattering cell. Prior to the measurements, the samples were kept at 22 and 40 °C, the desired measuring temperatures.

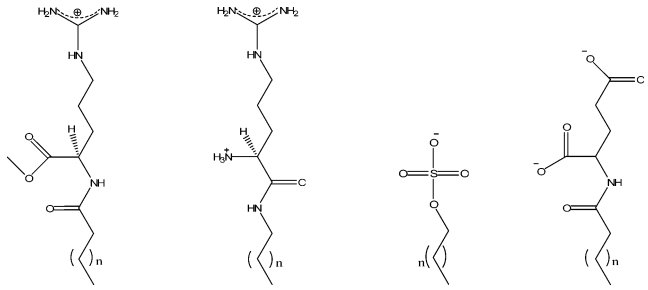

Figure 1. Chemical structures of the amphiphiles used in this study. Their names are listed in the following abbreviations: ALA for arginine-*N*-lauroyl amide dihydrochloride; LAM for N^{α}-lauroyl-arginine-methyl ester hydrochloride; SCS (SOS) for sodium cetyl (octyl) sulfate; and HS for sodium hydrogenated tallow glutamate.

Results

Spontaneous Vesicle Formation. Several catanionic vesicle systems composed of amino acid-based single-tailed surfactants are to be presented in this section. The chemical structures of the amphiphilic molecules used in this study can be seen in Figure 1. From left to right, we have LAM, ALA, SOS/SCS, and HS.

For mixed catanionic systems, the possibility of finding a region of net positively charged vesicles in the cationic surfactant-rich part, near the water corner, has been demonstrated in the literature.[6−8,46] A schematic representation of the water corner of a ternary phase diagram can be seen in Figure 2, where we have lobes representing the region where the cationic and anionic vesicles are expected to exist.

The fact that we are dealing with pseudoternary systems instead of true ternary ones should be pointed out. Actually, we have a five-component system in the sense of the Gibbs phase rule, and its representation should be pyramidal[47] instead of triangular. (The electroneutrality condition reduces the number of components to four.) Therefore, the pseudoternary phase diagram for S^+Cl^-, S^-Na^+, and water represents only a portion of the phase pyramid. The full pyramid is needed to represent

(43) Bellare, J. R.; Davis, H. T.; Scriven, L. E.; Talmon, Y. *J. Electron Microsc. Tech.* **1988**, *10*, 87−111.
(44) Adrian, M.; Dubochet, J.; Lepault, J.; McDowall, A. W. *Nature* **1984**, *308*, 32−36.
(45) Talmon, Y. *Ber. Bunsen-Ges. Phys. Chem. Chem. Phys.* **1996**, *100*, 364−372.
(46) Brasher, L. L.; Herrington, K. L.; Kaler, E. W., *Langmuir* **1995**, *11*, 4267−4277.
(47) Thalberg, K.; Lindman, B.; Karlstrom, G. *J. Phys. Chem.* **1991**, *95*, 6004−6011.

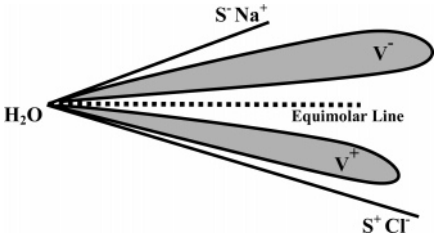

Figure 2. Schematic representation of the water corner of a pseudoternary phase diagram with oppositely charged surfactants. The gray lobe in the S^+-rich side represents the region of net positively charged vesicles.

compositions in multiphase regions where the surfactant ion and the associated counterion separate into different phases, as is the case when precipitates form. For clarity, we do, however, present the system as a pseudoternary phase diagram, emphasizing the part close to the water corner.

In a thorough search for the one-phase vesicle region for all systems, a large number of samples at different molar ratios of positively and negatively charged surfactants and different water weight percentages were prepared. However, no attempt to determine the complete phase diagram was included in this study. In the search for the samples containing vesicles, the observation that vesicle solutions have a bluish appearance[8,48] assisted the selection of the samples to be further characterized. Table 1 lists several samples studied and their corresponding compositions and provides some observations concerning the different structures that can be observed. The surfactant compositions are presented in molar concentration per charge, whereas the water content is presented in weight percentage; *R* represents the molar ratio between the cationic and anionic amphiphiles, which includes information on the excess positive charges in the surfactant mixtures.

The technique primarily used to investigate the aggregate structures in the different systems was cryo-TEM. The first system to be discussed, which corresponds to the first in Table 1, is the system LAM/SCS/W. Vesicles were found for all compositions presented in Table 1; however, the vesicles coexisted in solution with other kinds of structures: rodlike micelles, disks, and lamella (Figure 3).We denote by disks small lamellae, which, depending on their size and orientation, can be imaged by cryo-TEM as a circle, often with small contrast with the background, an ellipse or a straight bar.[49] The microcraphs in Figure 3 correspond to images taken from sample 1 (Figure 3b and c), sample 2 (Figure 3a), and sample 4 (Figure 3d). In samples 1 and 3, the presence of rodlike micelles and lamella in coexistence with vesicles was documented, whereas for samples 2 and 4, rods and disks were found instead. Samples with $R = 1.3$ and 99 or 99.5 wt % water were visualized by cryo-TEM with no structures seen.

Electrostatic forces are known to control the aggregation behavior of mixed ionic surfactant systems.[46] To illustrate this effect, we changed from one singly positively charged cationic surfactant to a doubly charged one, from LAM to ALA, respectively; the anionic surfactant was kept the same.

We expected that the vesicle lobe would be larger for the ALA-rich side because it is the shorter-chained surfactant. A one-phase region of vesicles was found for the system ALA/SCS/W at $R = 2.9$ and 99.5 wt % water (sample 8); see the cryo-TEM images in Figure 4c and d. Vesicles in coexistence with rodlike micelles were found for sample 5 (Figure 4a), sample 6 (Figure 4b), and sample 7; compositions are given in Table 1.

(48) Marques, E. F. *Langmuir* **2000**, *16*, 4798−4807.
(49) Almgren, M.; Edwards, K.; Karlsson, G. *Colloids Surf., A* **2000**, *174*, 3−21.

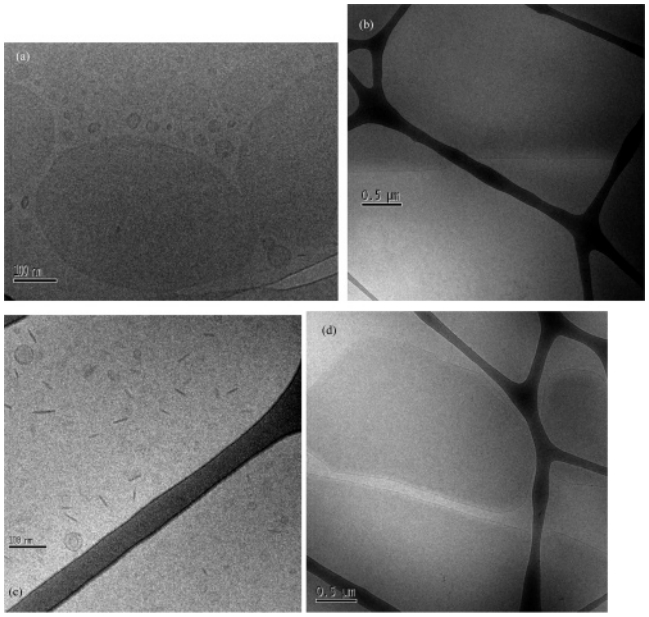

Figure 3. Cryo-TEM images of the system LAM/SCS/W. (a) Disks and small vesicles in coexistence obtained from sample 2; (b and c) images of a sample of system 1 where a lamellar structure, vesicles, and rodlike micelles can be seen; (d) image taken for sample 4, where vesicles can be seen coexisting with rodlike micelles.

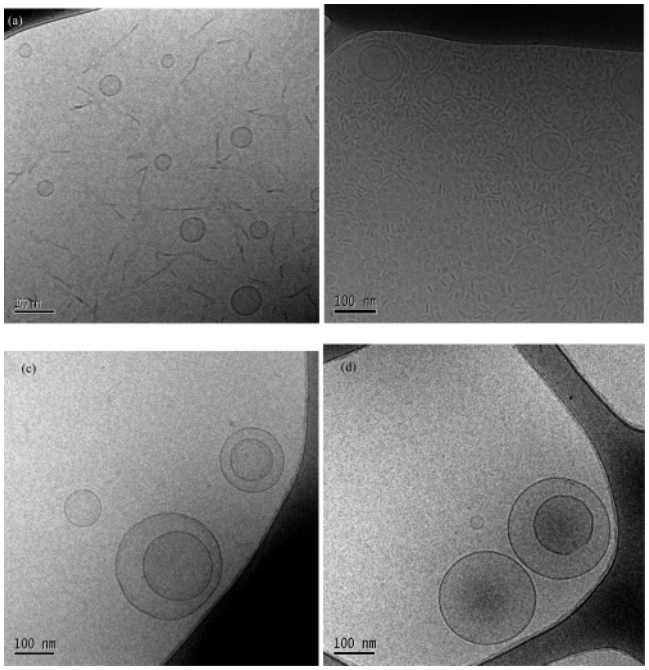

Figure 4. Cryo-TEM images of the system ALA/SCS/W. (a and b) Vesicles and rodlike micelles, samples 6 and 5, respectively; (c and d) unilamellar and multilamellar vesicle images obtained from sample 8.

The one-phase vesicle region found in sample 8 for this particular system was characterized with respect to polydispersity by monitoring a large number of vesicles in the cryo-TEM images taken. The size distribution was determined by measuring the diameter of each vesicle visualized in cryo-TEM. A population of 426 vesicles was analyzed. The number-average radius was calculated, giving a value of 80.9 nm; the size distribution is represented in Figure 5a. Taking into account that the thickness of the sample film in the cryo-TEM technique can go from 10 to 500 nm, we believe that our size distribution does not constitute an artifact affected by the range of sizes limited by the technique

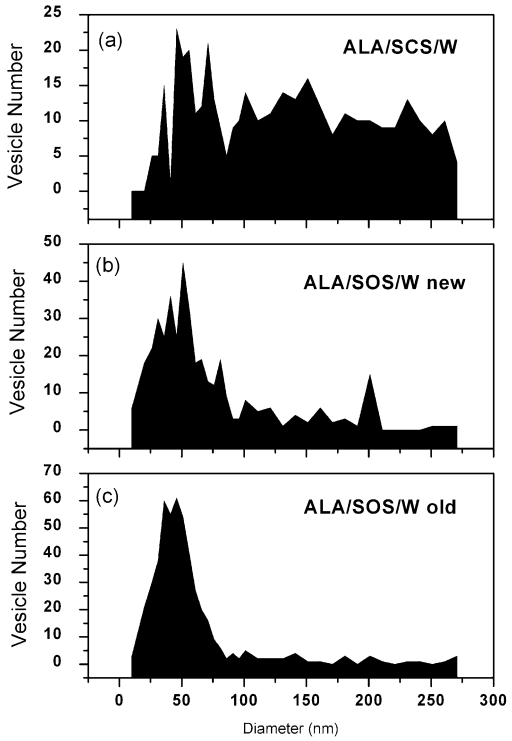

Figure 5. Vesicle size distributions obtained from cryo-TEM images taken for the systems (a) ALA/SCS/W, (b) an ALA/SOS/W 1-week-old sample, and (c) an ALA/SOS/W 240-day-old sample. A population of 426 particles was analyzed for the system containing SCS, and the number-average radius obtained was 80.9 nm. A population of 396 particles was analyzed for the 1-week-old sample containing SOS, and the number-average radius obtained was 35.5 nm. For the older ALA/SOS/W system, we obtained a number-average radius of 29.0 nm from measuring 479 particles.

but rather the real size distribution of the sample. However, it is possible that a few larger aggregates may be excluded during the process of creating a thin film of the sample.

We now consider the corresponding findings when we replaced the anionic amphiphile SCS by SOS. With this change, we aimed to address the effect of the surfactant hydrophobicity on the vesicle formation because SOS is less hydrophobic than SCS; the degree of chain asymmetry was kept the same in the sense that we still have a difference of four carbons between the two surfactant tails in the mixed system, from C12/C16 (ALA/SCS) to C12/C8 (ALA/SOS). The difference is that in the former system the cationic surfactant has the shorter chain whereas here it is the anionic; this does not seem to play a significant role in the ability to form vesicles because vesicles were visualized at $R =$ 1.7 for 98 (sample 9) and 99 (sample 11) wt % water. Cryo-micrographs of these samples can be seen in Figure 6: in part a, we can see vesicles and rodlike micelles coexisting (sample 12), and in parts b−d, we see vesicles of sample 11.

As for the system containing ALA and SCS, the vesicle size distribution was estimated for sample 11 by analyzing a population of vesicles within the cryo-TEM images taken. A population of 396 vesicles was analyzed. The number-average radius was calculated, giving a value of 35.5 nm. The vesicle size distribution can be seen in Figure 5b.

We will now turn to a discussion of the system where both surfactants are based on amino acids. In systems with glutamate-based anionic surfactant HS, we found vesicles at $R = 1.3$ and 99.92 wt % water. This can be seen in Figure 7a and b for the composition corresponding to sample 14 in Table 1; the imaging process was very difficult for this sample because of the strong

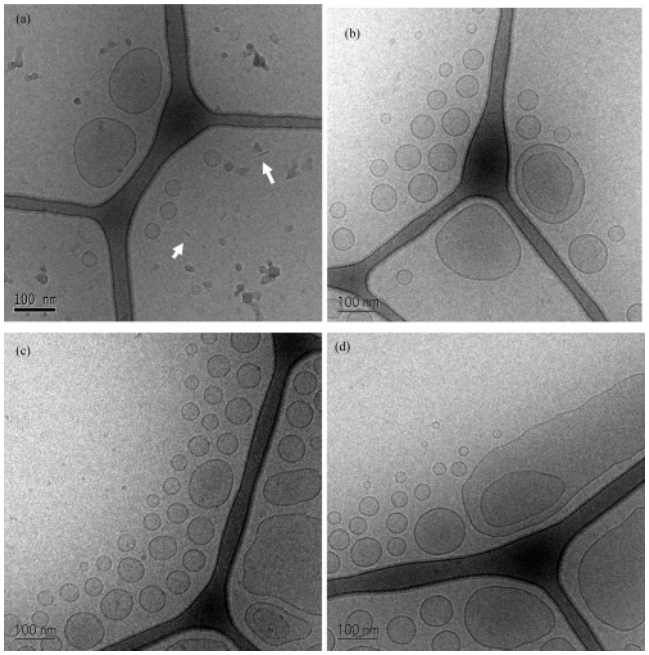

Figure 6. Cryo-TEM images of the system ALA/SOS/W. (a) Coexistence of vesicles with rodlike micelles obtained from imaging sample 12. (b−d) Unilamellar and multilamellar vesicle images obtained from sample 11. The white arrows indicate rodlike micelles.

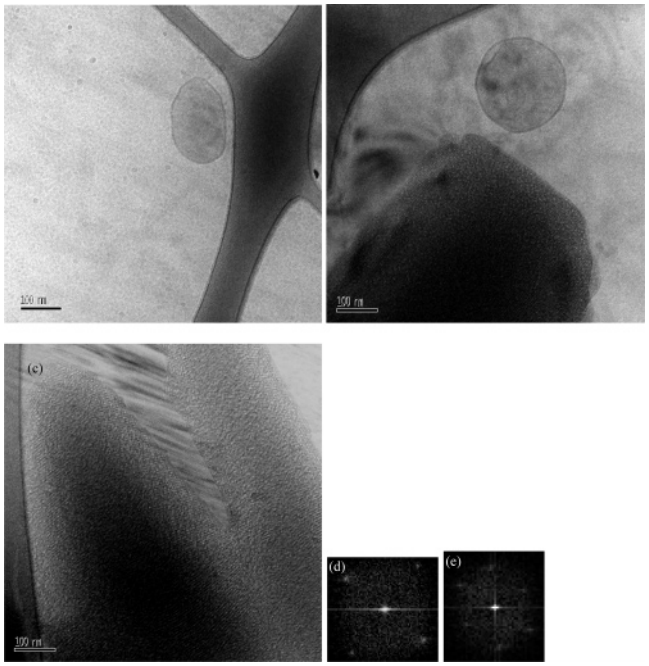

Figure 7. Cryo-TEM micrographs of the system ALA/HS/W, sample 14. (a−c) Vesicles and cubosomes and (d, e) fast Fourier transforms for the cubic particles.

beam sensitivity. Other structures were seen to coexist with the vesicles; their characteristics will be discussed later in the text.

Dynamic light scattering (DLS) experiments were performed for the vesicle system ALA/SCS/W, sample 8, with the intention of comparing the number-average radius obtained from the cryo-TEM images with the hydrodynamic radius, R_H. DLS is a technique that monitors the mean size of the particles through a mass-weighted distribution that favors larger sizes,[50,51] whereas cryo-TEM is a technique from which we get a number-average

(50) Egelhaaf, S. U.; Wehrli, E.; Muller, M.; Adrian, M.; Schurtenberger, P. *J. Microsc. (Oxford, U.K.)* **1996**, *184*, 214−228.

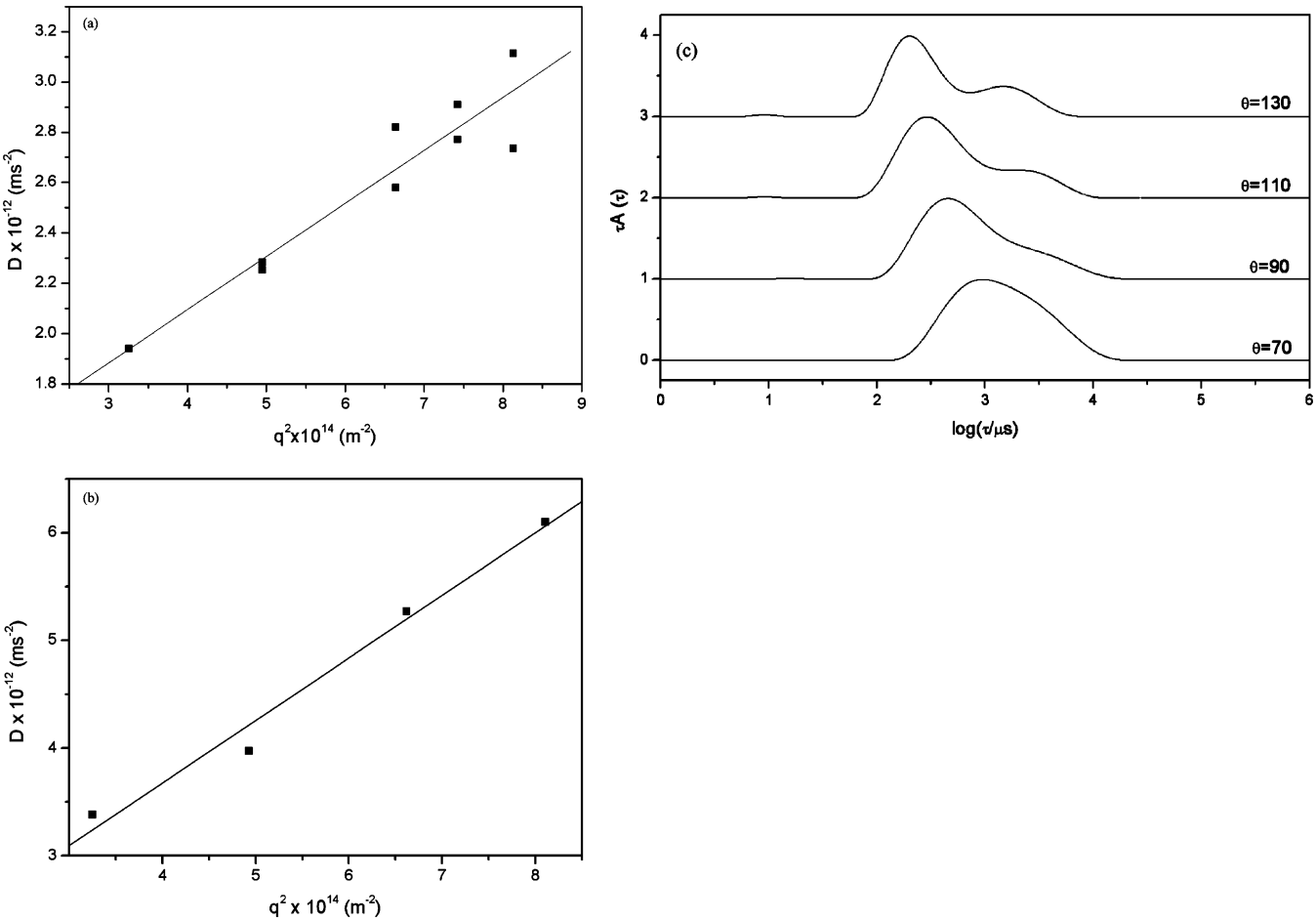

Figure 8. DLS results for the system ALA/SCS/W. (a) Apparent diffusion coefficients as a function of the square of the magnitude of the scattering vector for the sample at 22 °C; a hydrodynamic radius, R_H, of 181 nm was determined. (b) Apparent diffusion coefficients as a function of the square of the magnitude of the scattering vector at 40 °C; an R_H of 98 nm was determined. (c) Relaxation time distributions at different scattering angles and $T = 40$ °C.

radius that may favor smaller sizes because of the preparation method of the sample film.

Because of the high signal intensity obtained for the samples of the system containing ALA/SOS/W, the value of the hydrodynamic radius could not be properly determined; for the system ALA/SCS/W, we performed the experiments at 22 and 40 °C, and the results can be seen in Figure 8. No filtering or centrifugation of sample 8 was performed prior to DLS measurements so as not to affect the size distribution.

DLS measurements were performed at scattering angles of $\theta = 70$, 90, 110, 120, and 130° at 22 °C and $\theta = 70$, 90, 110, and 130° at 40 °C. The data were fitted to a single-exponential decay giving a mean average relaxation rate from which an apparent diffusion coefficient is calculated. Inverse Laplace transformations[52] were also used in the analysis.

The hydrodynamic radius (R_H) can be calculated using the Stokes−Einstein relationship $R_H = kT/(6\pi\eta_0 D)$, where k is the Boltzmann constant, T is the absolute temperature, and η_0 is the viscosity of the medium, which is water in this study.

In Figure 8a and b, we can see the plot of the apparent diffusion coefficients obtained at different angles versus q^2. From the extrapolation to zero q^2, we get apparent diffusion coefficients of 1.25×10^{-12} m^2 s^{-1} for the sample at 22 °C and 3.6×10^{-12} m^2 s^{-1} for the sample at 40 °C, corresponding to hydrodynamic radii of 181 and 98 nm, respectively.

The relaxation time distributions [$\tau A(\tau)$ vs $\log(\tau/\mu s)$] obtained from the regularized inverse Laplace transformation of the measured intensity time correlation functions at 40 °C are presented in Figure 8c. Polydispersity is shown by the width of the relaxation time distributions.

From the cryo-TEM experiments, we get a number-average vesicle radius of 80.9 nm, whereas with DLS, for the same temperature, we get a hydrodynamic radius of 181 nm. Thus, the DLS values are markedly higher than the cryo-TEM values, as expected.

Turbidity measurements made at room temperature and 40 °C for the same system, ALA/SCS/W (sample 8), show that we have higher turbidity for the samples at lower temperature (Figure 9). This feature could be related to a change from a multiple scattering regime of the sample to a normal scattering regime with increasing temperature or to a decrease in the particle size with temperature. However, taking into account the DLS results presented above, we believe that this increase in turbidity is due to an increase in vesicle size at lower temperature. Another feature of these turbidity experiments is that, independently of the system studied or the temperature at which it was performed, a clear decrease in turbidity with time is observed. In an attempt to understand this behavior better, we performed cryo-TEM for a 240-day-old sample of ALA/SOS/W (sample 11) and compared the vesicle size distribution with the one obtained for a 1-week-

(51) Coldren, B.; van Zanten, R.; Mackel, M. J.; Zasadzinski, J. A.; Jung, H. T. *Langmuir* **2003**, *19*, 5632−5639.
(52) Jansson, J.; Schillen, K.; Olofsson, G.; da Silva, R. C.; Loh, W. *J. Phys. Chem. B* **2004**, *108*, 82−92.

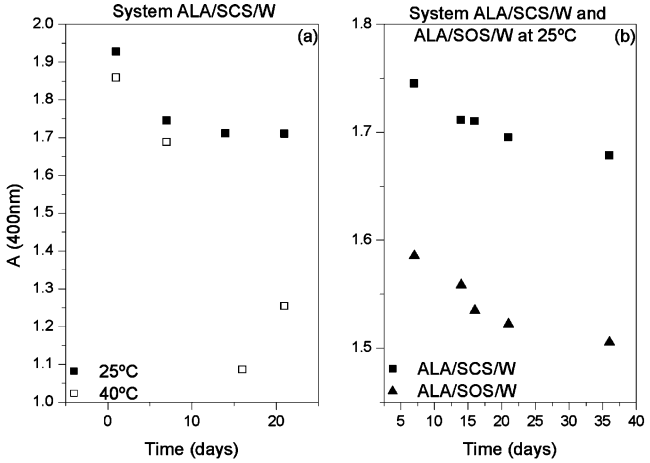

Figure 9. Turbidity experiments performed at 400 nm. (a) System ALA/SCS/W at 25 (■) and 40 °C (□). (b) Systems ALA/SCS/W (■) and ALA/SOS/W (▲). Both experiments were performed at room temperature.

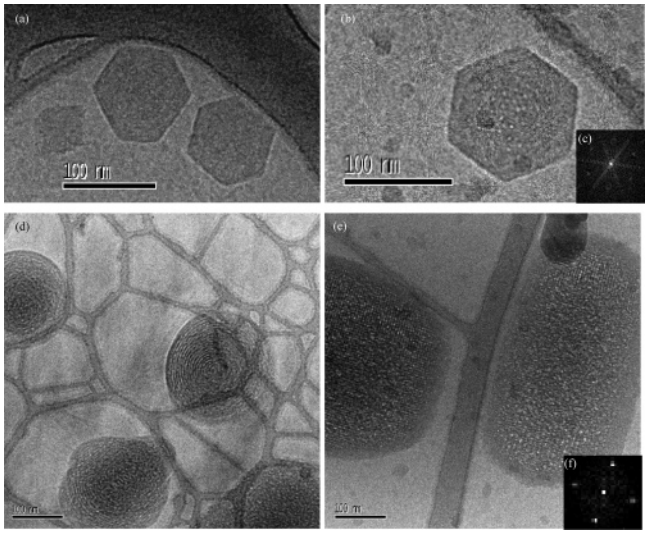

Figure 10. Cryo-TEM micrographs of the system ALA/HS/W, sample 13. (a and b) Cubosomes and (d and e) hexosomes are seen. (c and f) Fast Fourier transforms for the dispersed hexagonal and cubic dispersed particles, respectively, are shown.

old sample (Figure 5b and c, respectively). A change in the size distribution profile can be noted, with a shift toward a less polydisperse situation at longer times; a number-average radius of 28.9 nm has been calculated from the analysis of 479 individual vesicles, a clear decrease when compared with the value of 35.5 nm obtained with the 1-week-old sample.

Formation of Hexagonal and Cubic Structures. As mentioned above, an interesting finding in the search for a one-phase region of vesicles of the system of two amino acid-based surfactants (i.e., ALA/HS/W) for $R = 1.3$ and 99.92 wt % water (sample 14) was that of a different densely packed structure coexisting with the vesicles (Figure 7b and c). Fast Fourier transforms (FFTs) of the data of Figure 7b indicate a cubic structure aligned with the ⟨100⟩ plane parallel to the beam direction (Figure 7d). The FFT of an area in Figure 7c is shown in Figure 7e. This direction corresponds to a cubic phase aligned with the ⟨111⟩ plane parallel to the electron beam. From the particle morphology, we infer that the FFT in Figure 7e corresponds to a particle with a cubic structure, a cubosome. For the system ALA/HS/W (sample 13), the FFT of the dispersed particles obtained from the cryo-TEM images (Figure 10f) suggests that we are in the presence of the same cubic structures as found in sample 14.

In our examination of microstructures for the same system, we also found some well-defined hexagonally shaped particles. The FFT of the particle in Figure 10b indicates a hexagonal structure recorded along the ⟨001⟩ direction. The shape of the particles is very similar to that of dispersed particles with hexagonal symmetry, hexosomes, which has previously been reported.[31,53,54] The particles shown in Figure 10d also have hexagonal symmetry as previously demonstrated in the literature.[31−34,54]

Regarding the particle sizes, they range from 400 to 600 nm for cubic particles and from 100 to 200 nm for hexagonal particles.

The internal structure of the particles was partially destroyed during imaging because of the high beam sensitivity of the specimen. Therefore, the characterization and structure determination were difficult to make. Only small areas of the ordered particles could thereby be analyzed.

Discussion

Spontaneous Vesicle Formation. In mixtures of oppositely charged surfactants, the electrostatic contribution to the free energy of aggregation tends to favor aggregates with more nearly neutral charges,[46] leading to lamellar phases or solid crystals. However, when there is an excess of one of the amphiphiles, vesicles can form, especially if there is a difference in the length of the two hydrophobic tails.[55,56]

Studies presented in the literature on mixed catanionic systems in water predicted the existence of a region of net positively charged vesicles in the cationic surfactant-rich side, near the water corner, and they also predicted the possibility of spontaneous vesicle formation.[6−8,46]

For the system containing LAM and SCS, vesicles were found for all compositions investigated; however, as mentioned in the Results section, they coexist in solution with other kinds of structures: rodlike micelles, disks, and lamella (Figure 3). The coexistence between vesicles and lamellas and/or rodlike micelles has been previously reported in studies of catanionic systems in the fluid state.[7−10,46] Studies done on the gel state of catanionic systems have also shown vesicle formation with an excess of one of the surfactants; these vesicles were faceted, the appearance of facets being attributed to a coexistence between molten and crystallized bilayers within the catanionic vesicles.[57,58] A theory predicting the coexistence of vesicles and disks, where during cocrystallization an excess of one of the surfactants accumulates on the edges or pores rather than being incorporated into the crystalline bilayers, has also been presented.[59]

Asymmetry in the tail chain length has been shown to favor vesicle formation in compositions rich in the surfactant with the shorter tail.[7,8,60] Thus, we were expecting to find the one-phase vesicle region easily for the LAM/SCS/W system, which was not the case. Although we could visualize vesicles for a range

(53) Monduzzi, M.; Ljusberg-Wahren, H.; Larsson, K. R. *Langmuir* **2000**, *16*, 7355−7358.
(54) Almgren, M. *Aust. J. Chem.* **2003**, *56*, 959−970.
(55) Yuet, P. K.; Blankschtein, D. *Langmuir* **1996**, *12*, 3819−3827.
(56) Yuet, P. K.; Blankschtein, D. *Langmuir* **1996**, *12*, 3802−3818.
(57) Vautrin, C.; Dubois, M.; Zemb, T.; Schmolzer, S.; Hoffmann, H.; Gradzielski, M. *Colloids Surf., A* **2003**, *217*, 165.
(58) Vautrin, C.; Zemb, T.; Schneider, M.; Tanaka, M. *J. Phys. Chem. B* **2004**, *108*, 7986−7991.
(59) Dubois, M.; Lizunov, V.; Meister, A.; Gulik-Krzywicki, T.; Verbavatz, J. M.; Perez, E.; Zimmerberg, J.; Zemb, T. *Proc. Natl. Acad. Sci. U.S.A.* **2004**, *101*, 15082−15087.
(60) Safran, S. A.; Pincus, P.; Andelman, D. *Science* **1990**, *248*, 354−356.

of compositions, the vesicles were always in coexistence with other self-assembly structures.

On changing from a singly positively charged cationic surfactant to a doubly charged one, from LAM to ALA, there are notable changes: the phase behavior seems to be simplified because we find vesicles coexisting with rodlike structures alone.

Again, we expected that for the system containing SCS, the vesicle lobe, if it existed, would be larger for the ALA-rich side because this is the shorter-chained surfactant. In fact, as mentioned in the Results section, a one-phase region of vesicles was found for the system ALA/SCS/W at $R = 2.9$ and 99.5 wt % water (sample 8); for the other samples characterized, vesicles were found to coexist with rodlike micelles (samples 5−7). This is an indication of the electrostatic influence on the phase behavior of the catanionic mixtures with facilitated vesicle formation.

By replacing SCS with SOS, we illustrate the role of the hydrophobic effect on vesicle formation. To make it clearer, we used similar chain asymmetry by going from a C_{12}/C_{16} to a C_{12}/C_8 S^+/S^- tail-length ratio. Vesicular structures were found at R = 1.7 and 98 (sample 9) and 99 (sample 11) water weight percentages. For samples 10 and 12, vesicles were found to coexist with rodlike micelles. The fact that we found a one-phase vesicle region at 98 wt % water and above, for a fixed ratio between the cationic and anionic surfactants, indicates that this system has a larger cationic vesicle lobe than all of the other systems presented so far. It seems that the presence of a shorter-chained surfactant induces better packing of the tails within the bilayer and softens the membrane. Yuet and Blankschtein[55] developed a theory that was applied to describe vesicle formation in the cetyltrimethylammonium bromide/sodium octyl sulfate, CTAB/SOS, system. In this theory, the free-energy terms include the contributions of the surfactant-tail packing, the steric interactions of the surfactant headgroups, and the electrostatic interactions between oppositely charged surfactant heads. The application of this theory to describe the effect of the surfactant tail length showed that surfactant tail-length asymmetry between the two components has a vesicle stabilizing effect. The shorter tails can fit nicely into the space near the outer hydrocarbon−water interface without protruding deeply into the hydrophobic region. Consequently, the 8-carbon chain surfactant used, SOS, would cover the outer interface without interfering significantly with the packing environment of the 12-carbon chain from ALA in the hydrophobic interior, thus facilitating the formation of curved surfaces and hence vesicle formation.

For the system containing ALA and HS, vesicle structures were also found (sample 14, Figure 7a and b). However, a different densely packed structure was found to coexist with them; a discussion of this structure will be presented below. A one-phase region of vesicles alone was not found, and we believe that this can be attributed to the particular characteristics of the two surfactants: they are both doubly charged, and HS has the highest degree of hydrophobicity of all of the amphiphiles used in this study.

Above, we stated that an unequal partitioning of the surfactant electric charges between the outer and inner layers of the particle takes place in the formation of the catanionic vesicles.[55] This possibility raises the following question: what is the role of excess surfactant in vesicle formation and stability for the catanionic vesicles? If we consider that with an excess of one of the surfactants the vesicles will have a net charge, then this net charge will give rise to electrostatic vesicle−vesicle repulsion and thus increase the stability of the vesicles in the solution. The net charge will also control the interactions with oppositely charged polyelectrolytes with phase separation occurring near charge neutralization.[61]

Another interesting subject that can be addressed and, in general, creates a considerable amount of controversy is whether these catanionic vesicles can be considered to be thermodynamically stable structures or not. Their spontaneous formation is a strong indication of their stability. However, other features also have to be considered:[48,62] there should be stability in time with respect to the size distribution if equilibrium is reached; the formation and properties of vesicles have to be reversible upon changing an external factor and independent of the method of preparation; and they should be in equilibrium with neighboring single-phase regions in the phase diagram. Some of these criteria are difficult to address experimentally. The one related to the equilibrium of vesicles with neighboring single-phase regions in the phase diagram could be experimentally tested. Here we will consider only the vesicle size distribution for the systems ALA/SCS/W and ALA/SOS/W as well as the time dependency of this size distribution.

Size distributions obtained from cryo-TEM images are known to shift toward smaller radii while DLS experiments yield a size distribution that shifts toward larger particles.[50,51] Furthermore, cryo-TEM images correspond to a projection of the particles in the image plane and are believed to provide close to the real bulk distributions[50,51] as long as the particle size is within the resolution limit of the technique. As stated above, we believe this to be the case for both systems considered here (i.e., ALA/SCS/W and ALA/SOS/W).

The vesicle size distributions were estimated by analyzing a population of vesicles within the cryo-TEM images. For the vesicles with SCS, a number-average radius of 80.9 nm was obtained, whereas for the vesicles with SOS, we got a value of 35.5 nm (Figure 5b). The system containing SCS was highly polydisperse when compared with the SOS system. It has been shown previously that vesicles formed by catanionic surfactant mixtures of unequal chain length are typically polydisperse.[63] In a study by Coldren et al.,[51] it has been shown that the stiffer (higher bending constant, K) the bilayer the less polydisperse the vesicle sample; these authors determined the sum of the Helfrich bilayer elastic parameters and the spontaneous curvature radius from the size distribution obtained from the cryo-TEM images for three different systems. Relating their results to ours, we can infer that the vesicle system composed of ALA and SOS probably has higher bilayer stiffness than that composed of ALA and SCS, resulting in a less polydisperse size distribution as can be seen in Figure 5b.

As expected, the vesicle size determined by DLS was larger than the one obtained from cryo-TEM analysis; we got a value of 181 from DLS and a value of 80.9 from the cryo-TEM analysis for the same temperature.

A decrease in the hydrodynamic radius for the vesicles of the system ALA/SCS/W from 181 to 98 nm was found when increasing the temperature from 22 to 40 °C. Turbidity measurements confirmed that the particles are smaller at higher temperature. Moreover, we noted a decrease in turbidity with time, which made us compare the vesicle size distribution of a 1-week-old sample with that of a 240-days-old one (Figure 5b and c). A change in the number-average vesicle radius with time from 35.5 to 28.9 nm has been determined. Similar observations have been made before by Kaler et al.[7] and have been related

(61) Marques, E. F.; Regev, O.; Khan, A.; Miguel, M. D.; Lindman, B. *Macromolecules* **1999**, *32*, 6626−6637.
(62) Laughlin, R. G. *Colloids Surf., A* **1997**, *128*, 27−38.
(63) Jung, H. T.; Coldren, B.; Zasadzinski, J. A.; Iampietro, D. J.; Kaler, E. W. *Proc. Natl. Acad. Sci. U.S.A.* **2001**, *98*, 1353−1357.

to the effect of mixing on the local surfactant concentration. The vesicle size is expected to depend on composition, with the bilayer curvature decreasing as a near-equimolar composition is approached. Therefore, procedures with poor mixing, such as ours, produce widely varying local compositions and a correspondingly wide distribution of sizes initially. In a study by Marques,[48] where the size and stability of catanionic vesicle systems were analyzed with respect to varying preparation method and aging, it was shown that different preparation paths for an identical bulk composition lead to the formation of the same type of self-assembled structures but that the size and polydispersity of the vesicular aggregates varied between the different preparation paths. Because the polydispersity is related to different metastable states, the equilibrium size distribution may not be easily reached and then only at an extremely slow rate. Hao et al.,[64] however, have shown that catanionic vesicles, with an excess of the cationic surfactant, correspond in the very dilute region to nonequilibrium structures. These authors demonstrated that vesicles form spontaneously in extremely dilute catanionic surfactant systems if one of the components is produced by an in-situ chemical reaction rather than by mixing of the components, thus avoiding the influence of shear-stress forces, and that the resultant vesicle phase is a thermodynamically stable state. Almgren[54,65] also argues that truly equilibrated vesicles should have a size distribution that is independent of the history of the sample.[65] Only if that holds true can the various theories for the size of equilibrium vesicles be tested,[65] and he notes that there is nothing to indicate that vesicles are anything but a dispersion of the lamellar phase.

As a summary of this discussion and keeping in mind the fact that we managed to demonstrate vesicles for all systems presented, we can infer that the stability of these catanionic vesicles is ensured by the excess of one the surfactants and that the vesicles form spontaneously and remain stable for long periods of time.

Particles with Hexagonal and Cubic Internal Structures. A notable finding of this investigation of particles in mixed systems of amino acid-based surfactants is that of dispersed particles with cubic and hexagonal internal structures, namely, cubosomes and hexosomes. The cubosome particles were found to coexist with vesicle structures for sample 14, which seems to be a common behavior for these systems,[30,53] and with hexosomes for sample 13.

The shape of the particles in Figure 10d can be compared with similar structures found in the literature when reporting on hexosomes.[31−34,54] According to these references, the particles consist of a bundle of cylinders bent by 180°, as can be seen in the Figure. These particles formed spontaneously, and no stabilizer was added to disperse them in solution.

These findings are significant because cubic dispersed particles have recently been the subject of a great number of studies because of their interesting internal structure and their considerable potential from an application point of view.[18] They are even more interesting in our case because they form without adding any stabilizer, which otherwise is a common feature of these systems.[28,30,32−34,53,66]

Conclusions

The spontaneous formation of vesicles as well as particles with cubic and hexagonal internal structures has been reported for catanionic amino acid-based surfactant systems. A balance between electrostatics and hydrophobic interactions contributes to the final structures formed. The spontaneous formation of vesicles is favored by electrostatics and an alkyl chain asymmetry, whereas a decrease in the degree of hydrophobicity gives an additional flexibility to the bilayers. The size distribution profiles of vesicles are presented for mixed systems of arginine-based surfactants and two classical anionic surfactants; a considerable degree of polydispersity is found. The size distribution profile is found to become more narrow, and the number-average radius is lower with time. Previously it was shown that the size distribution depends on the preparation method.[48] The solutions are found to remain vesicular for very long periods of time.

The presence of particles with internal cubic and hexagonal structures is demonstrated from fast Fourier transforms of the cryo-TEM images for a mixed system of one anionic and one cationic amino acid-based surfactant. The particles appear to correspond to the cubosomes and hexosomes presented in the literature. They form spontaneously, and no stabilizer needed to be added for their formation. The ease of formation and stability of these particle dispersions opens them to a broad range of applications, such as candidates for drug-delivery systems in particular because these surfactants are found to have low toxicity and to be biodegradable.

Acknowledgment. We are grateful to Viveka Alfredsson for help with the FFT analysis, to Gunnel Karlsson for assistance with cryo-TEM instrumentation, and to Telma Costa and Karin Schillén for help with the DLS experiments. We also acknowledge Mats Almgren for helpful suggestions and Kåre Larsson, Otto Glatter, and Fredrik Tiberg for fruitful discussions. This work was supported by grants from the Fundação para a Ciência e Tecnologia (FCT, projects POCTI SFRH/BD/8357/2002, FEDER-POCTI/QUI/58689/2004, and POCTI/QUI/45344/02), the Swedish Research Council (VR), and a grant from an EU Research Training Network, CIPSNAC (contract number MRTN-CT-2003-504932).

LA053464P

(64) Hao, J. C.; Yuan, Z. W.; Liu, W. M.; Hoffmann, H. *J. Phys. Chem. B* **2004**, *108*, 5105−5112.

(65) Almgren, M.; Rangelov, S. *Langmuir* **2004**, *20*, 6611−6618.

(66) Johnsson, M.; Barauskas, J.; Tiberg, F. *J. Am. Chem. Soc.* **2005**, *127*, 1076−1077.